universe

MDPI

Article

Present and Future of $0\nu2\beta$ Searches with Germanium

Nina Burlac and Giuseppe Salamanna *

Department of Mathematics and Physics, Roma Tre University and INFN Roma Tre, 00146 Rome, Italy; nina.burlac@uniroma3.it

* Correspondence: giuseppe.salamanna@roma3.infn.it

Abstract: Among the several experiments and techniques conceived of to search for neutrinoless double β decay ($0\nu2\beta$) in a handful of isotopes, presently the best lower limit on the half-life for this rare process, is provided by those using ^{76}Ge, a rare isotope of germanium. Such a lower limit is of 1.8×10^{26} y. Building from such a successful achievement of the GERDA and Majorana Demonstrator experiments, the baton with ^{76}Ge passes now to the LEGEND experiment. Using a two-stage approach with about 200 kg and then 1 t of germanium, LEGEND aims to attain a sensitivity of around 10^{28} y, which will enable it to probe the standard inverted-ordering neutrino mass scenario. We touch upon the past generation of experiments to illustrate their strong and weak points, review the general concept and design of LEGEND, and describe the LEGEND-200 detector and its preliminary performance. We also illustrate how the backgrounds can have a dramatic effect on the search and in which way the latter can be mitigated.

Keywords: germanium; $0\nu2\beta$; GERDA; Majorana; LEGEND; ton scale

check for updates

Citation: Burlac, N.; Salamanna, G. Present and Future of $0\nu2\beta$ Searches with Germanium. *Universe* **2021**, *7*, 386. https://doi.org/10.3390/universe7100386

Academic Editor: Maria Vasileiou

Received: 15 September 2021
Accepted: 11 October 2021
Published: 18 October 2021

Publisher's Note: MDPI stays neutral with regard to jurisdictional claims in published maps and institutional affiliations.

Copyright: © 2021 by the authors. Licensee MDPI, Basel, Switzerland. This article is an open access article distributed under the terms and conditions of the Creative Commons Attribution (CC BY) license (https://creativecommons.org/licenses/by/4.0/).

1. Introduction

In this Special Issue on "Neutrino-less Double Beta Decay" ($0\nu2\beta$), several experiments are reviewed, which search for Lepton Flavor Violation (LFV) in the neutrino sector by looking for such a rare process. This decay would occur only if the only a known neutral elementary particle, the neutrino, coincides with its own antiparticle (the antineutrino) by virtue of the Majorana condition applying to its mass in the Standard Model (SM) Lagrangian. The experiments are based on a handful of techniques that rely on different signal carriers and, consequently, specific detector layouts to achieve the scope. There are other experiments that are expected to have comparable sensitivities to those described in this review. It is worth mentioning here one based on bolometry in ^{100}Mo (CUPID) [1] and one based on a liquid xenon time projection chamber with ^{136}Xe (nEXO) [2].

One of the most consolidated techniques is based on the energy measurement of the two-electron final state in a polarized semiconducting diode made out of germanium. A particular isotope of this common semiconductor, ^{76}Ge, has a peculiar arrangement of its nuclear energy levels, and therefore, it can undergo double β decays. The story of the search for $0\nu2\beta$ with germanium diodes is long, having originated in the late 1960s from an idea of E. Fiorini [3]. The International Germanium EXperiment (IGEX) [4] at Canfranc and the Heidelberg–Moscow experiment [5] at LNGS advanced the search using detectors enriched in ^{76}Ge. When it became possible to put together larger masses of germanium, this resulted in the latest generation experiments, GERDA and Majorana Demonstrator. While $0\nu2\beta$ has not been observed as of yet, in the past decade, this technique has yielded the most stringent lower limit on its half-life to date. The GERDA experiment at Laboratori Nazionali del Gran Sasso (LNGS) of Istituto Nazionale di Fisica Nucleare (INFN), in Italy, has run for several years, establishing a lower limit of 1.8×10^{26} y with a Confidence Level (C.L.) of 90% [6]. Its competitor based in the USA, the Majorana Demonstrator (MJD), has published a competitive figure, confirming the suitability and reliability of germanium diodes for the purpose at hand.

Based on this successful past, the "germanium community" has joined forces to build the next-generation experiment "LEGEND", which will take the technique to the ton scale and approach the half-life range of 10^{28} y. Failure to observe $0\nu2\beta$ at this reference value would lead to excluding that neutrino masses are organized according to the so-called "inverted" ordering. LEGEND will follow a two-stage approach. The first stage, with 200 kg of germanium enriched in ^{76}Ge at about 88%, will exploit the GERDA layout in minimizing the backgrounds plus the MJD high-energy resolution. This phase will be held at LNGS and will use the GERDA infrastructure, suitably improved. The next step will use a ton of germanium enriched at 91%. This second stage, LEGEND-1000, will need to meeting the goal of the considerable reduction of the background rate (about a factor 50 less than GERDA): this will require improvements and creativeness in almost all the experimental ingredients.

Several comprehensive reviews on the subject have been written in the past, e.g., [7]. The present review builds on those, but aims at putting the focus especially on the future and wishes to provide updated figures on the state-of-the-art and outlook. We first elaborate on what GERDA and MJD have been: their different strategies, a summary of their technical features, and a recap of their final performance. Then, we illustrate the present, with LEGEND-200, its current status, and what has been changed or improved with respect to its "parents". A discussion of the most important technological advancements in designing LEGEND-1000 is offered, with the narrative aimed at showing how those are meant to tackle each separate background source in order to reduce it at or below the desired level. We decided to focus on the experimental landscape and take for granted that the reader is familiar with the theoretical framework and the basics of the experimental signature. Therefore, here, we talk only briefly about the relationship between the measured half-life and the Majorana effective mass $m_{\beta\beta}$, the relation with the mass ordering, and the question of the Nuclear Matrix Element (NME) and its computation for the various isotopes according to different nuclear models.

The paper structure is as follows: in the first section, the physics relations and a reminder of the NME range of values for germanium are given; then the "parent" experiments are described and the state-of-the-art presented, with emphasis on the working principle of germanium diodes. Then, we proceed to describe in more detail the LEGEND-200 apparatus and its expected performance, with an eye on the mitigation of the main backgrounds. The last section is devoted to LEGEND-1000 and how it is expected that it can attain a significant background reduction.

2. Basics, Mathematical Relations, Mass Ordering, and the NME

The Majorana effective mass $m_{\beta\beta}$ is a squared-amplitude parameter with the dimension of a mass, whose definition from the Pontecorvo–Maki–Nakagawa–Sakata (PMNS) matrix elements U_{ei} and neutrino eigenstate masses m_i is:

$$m_{\beta\beta} = |\sum_{i=1}^{3} U_{ei}^2 m_i| \quad (1)$$

where U_{ei} includes also the Majorana phases λ_1 and λ_2. The mathematical relation between the observable half-life of a nuclear isotope ($T_{1/2}^{0\nu}$) and the square of $m_{\beta\beta}$ is of inverse proportionality, through a Nuclear Matrix Element (NME), $M_{0\nu}$, which encompasses the nuclear Hamiltonian terms of the double β decay:

$$(T_{1/2}^{0\nu})^{-1} = G_{0\nu} M_{0\nu} \langle m_{\beta\beta} \rangle^2 \quad (2)$$

with $G_{0\nu}$ representing the phase space factor for the kinematics of the decay [8]. For relatively high mass isotopes, $M_{0\nu}$ is difficult to compute, because of the potential energy among the many nucleons. To compute it, one has to rely on approximated nuclear models. The premises of the various models and the approximations implied result in numerical values for the predicted NME, which, in some cases, differ by over 100%. A review of the

values for various isotopes can be found in [9]. Specifically for ^{76}Ge, the NME computed in various schemes differs by as much as over a factor two between the lowest and the highest. This is similar to other isotopes.

The explicit expression of $m_{\beta\beta}$ in Equation (1) depends on whether the neutrino eigenstates are ordered directly or inversely (see for example [10]). Therefore, $0\nu2\beta$ searches are sensitive to the neutrino mass ordering, provided that the lightest neutrino eigenstate is light enough ($m_{\text{light}} \lesssim 5 \cdot 10^{-2}$ eV). Depending on the NME value one picks, for example for ^{76}Ge, a lower limit on $T^{0\nu}_{1/2}$ translates into an upper limit on $m_{\beta\beta}$ and, in turn, allows ruling out regions of probability for the inverse ordering. This is illustrated in Figure 1, from [11]. $T^{0\nu}_{1/2} \approx 10^{28}$ y is the value where direct and inverted ordering are well separated, in the lowest m_{light} region. The question was put in context and correctly spelt out, e.g., in [10]. In the middle and rightmost parts of Figure 1, $m_{\beta\beta}$ is shown as a function of the quantity Σ and m_β, respectively. Σ represents the sum of the masses of the three neutrino eigenstates, as measured by cosmological observations deduced from the gravitational effects of free-streaming neutrinos in the early Universe. The upper limits of 0.12 eV and 0.66 eV are obtained on Σ, which both depend on some assumptions on the modeling of the evolution of the Universe [12]. A totally model-independent approach to the extraction of the neutrino masses is taken from measuring the electron neutrino mass in β decays of tritium; the one shown is $m_\beta < 0.23$ eV, the 5 y sensitivity of the KATRIN experiment [13].

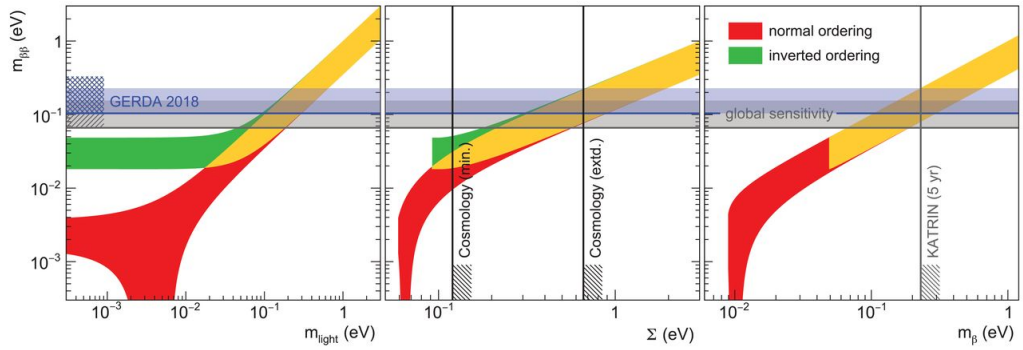

Figure 1. Constraints on the quantity $m_{\beta\beta}$ are shown, left to right, as a function of the lightest neutrino mass, the sum of neutrino masses, and the effective neutrino mass measured in β decays. The blue horizontal band shows the upper limits on $m_{\beta\beta}$ obtained by GERDA in 2018 (104–228 meV, depending on the NME value considered); the gray band shows those from combining the sensitivities of all leading experiments in the field. Taken from [11].

3. Germanium Diodes

3.1. The Experimental Signature in Germanium

^{76}Ge undergoes $0\nu2\beta$ via the process $^{76}Ge \rightarrow {}^{76}As + 2e^-$, where the observable is the sum energy released by the two electrons in the detector, this is as for all $0\nu2\beta$, a single line in the spectrum, broadened by the limited detector energy resolution. The Q-value for the above reaction in ^{76}Ge is $Q_{\beta\beta}$ = 2039 keV. The search focuses on a region of interest around this value. At its lower end, the counts in the spectra will be dominated by the standard double β decay, which has a decay width of at least five orders of magnitude larger than the supposed $0\nu2\beta$ but characterized by the typical broad β decay distribution. It follows that the most important figures of merit to maximize the statistical sensitivity to $0\nu2\beta$ are the following:

- Exposure of the relevant isotope (^{76}Ge), which means high mass and/or long data taking time;
- Energy resolution to disentangle the $0\nu2\beta$ peak at the end-point of the di-electron energy spectrum from the ordinary double β decay;
- An as low as possible count of background events in the Region Of Interest (ROI) around $Q_{\beta\beta}$.

The statistical sensitivity in the presence of the background is parameterized as follows:

$$S \propto \varepsilon \times f \times \sqrt{\frac{M \times t_{run}}{B \times \Delta E}} \quad (3)$$

where S is the sensitivity, ε is the experiment efficiency to $0\nu2\beta$ events, f is the isotopic abundance within the chemical element of the sample, M is the overall mass of the sample, t_{run} is the effective data taking time, B is the so-called background index, while ΔE is the energy resolution at $Q_{\beta\beta}$. The isotopic abundance f of ^{76}Ge in natural germanium is low, about 7%. However, it is possible to enrich a detector in ^{76}Ge to about 88%, which is what has been done for the past experiments and is being done for LEGEND-200. The most recent techniques allow advancing this percentage further to above 90%, a measure that is being pursued in view of LEGEND-1000. The background index B is defined as the number of background counts in the ROI and can be expressed through its relation to the absolute number of background events included in the $0\nu2\beta$ search region:

$$N_{bkg} = M \times t_{run} \times B \times \Delta E \quad (4)$$

3.2. The Detection Technique

In the case of germanium-based experiments, the electron energy, released by ionization in the semiconducting diodes, generates a current of charge carriers. This, in turn, is collected on an electrode, connected to a front-end electronics, which reads the current signal and records it. Different geometrical and electric field configurations have been developed for use in the GERDA and MJD experiments, which are described below.

3.3. Types of Diodes

Four types of diodes have been developed that are being applied to the $0\nu2\beta$ experiments: coaxial and Broad-Energy Germanium (BEGe, in GERDA), the P-type Point Contact (PPC, in MJD), and the Inverted Coaxial Point Contact (ICPC), which is going to have the lion's share in LEGEND. We dwell on the latter, describing its features and how it improves the experiment performance with respect to the other configuration.

3.3.1. ICPC

The ICPC concept was first introduced in [14]. Well over 100 kg of the germanium detector in LEGEND-200 are of this type. It is a p-type diode with a cuboid shape of 80 mm to 100 mm sides. It is a point-contact, which means that the charge or hole originating from the di-electron energy release is driven to a p^+ electrode, implanted with boron. The diode is reversely polarized, that is the rest of its outer surface is effectively a 0.7 mm-thick n^+ electrode, to which a polarization potential is applied (≈5 kV) and over which lithium is diffused. Negative charges drift towards the n^+ polarity, while holes are attracted towards p^+. The electrodes are electrically isolated by means of two grooves on each side of the p^+ point. Those etched grooves and the p^+ point itself are the only thin-enough barriers (about 0.3 µm thick) through which outside heavier particles, such as α, can penetrate into the germanium active region. This constitutes a dangerous background for the $0\nu2\beta$ search.

Currently, detectors of a mass up to 2 kg each have been constructed, by growing germanium crystals from powder with the Czochralski method. In the future, masses of 2.6 kg on average are expected to be reached for LEGEND-1000. A single, large mass detector is desirable over many small solids for a variety of reasons:

- First of all, because this minimizes the amount of front-end electronics and cables to read its signals, which are a source of radioactive background very close to the $0\nu2\beta$ site;
- Furthermore, a reduced surface-to-volume ratio thus achieved significantly diminishes the rate of α and β radiation, since they only make it through via fixed-surface p^+ contacts and the grooves;
- Finally, this is more cost-effective.

A characterization of the ICPC for future use was performed by GERDA and is documented in the newly published [15].

The ICPC has this one stark advantage of being more massive with respect to BEGe and the PPC. All three are otherwise substantially equivalent in performance, in that all of them ensure a suitably stable electric field configuration across the inner germanium volume, such that the weighting potential, the solution of the Laplace equation, is also uniform. This is a highly desirable feature, because it allows treating most of the volume in a single way. In turn, this helps with rejecting background particles, which interact diffusely along their path through the germanium volume (Multi-site Event) (MSE)). $0\nu2\beta$ decays will manifest as so-called Single-Site Events (SSEs), instead, with a single point of energy release from which the drift originates. This is nicely illustrated in the cartoon of Figure 2, from [11].

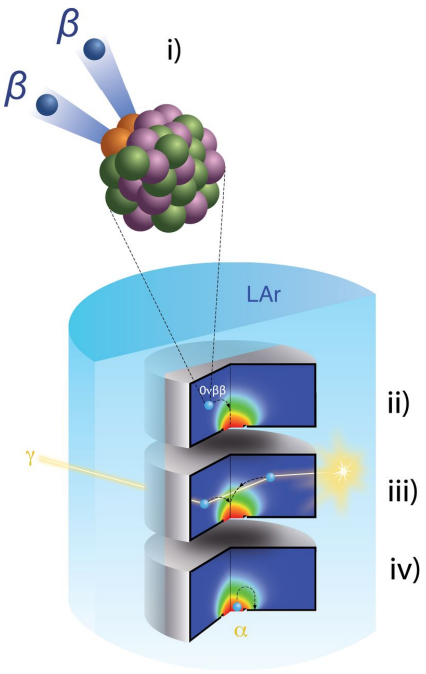

Figure 2. (i) Artist's view of the $0\nu2\beta$ of a nucleus by an emission of two electrons. (ii–iv) Three BEGe detectors from the GERDA detector, immersed in liquid argon (light blue cylinder). Events from $0\nu2\beta$ would deposit all $Q_{\beta\beta}$ energy within a few cubic millimeters in a single detector (ii). Events with coincident LAr scintillation light or with multiple interactions in the diode (e.g., from Compton scattering (iii)) are classified as background events. Similarly, α decays at the readout electrode show unique signal characteristics (iv). Taken from [11].

Different from the ICPC, BEGe, and the PPC, the old coaxial detector used in GERDA has a rapidly changing weighting potential within its space. The main difference comes from the fact that the coaxial uses an extended p^+ contact along an internal slim cylindrical aperture coaxial to the outer surface (hence the name). This geometrical configuration renders the above task more complicated and the resulting background rejection less effective. The reduced electrode size of point-contact detectors also results in a smaller capacitance, which in turn means they have a better intrinsic energy resolution than the extended coaxial electrodes.

For these reasons, LEGEND-200 will not use coaxial detectors at all in its arrays. It will recycle about 60 kg of BEGe and the PPC from its parent experiments.

3.3.2. Pulse Shape Discrimination: How It Works in the ICPC

Pulse Shape Discrimination (PSD) algorithms allow exploiting the different topology of $0\nu2\beta$ and backgrounds in the diode to reduce the latter. GERDA and MJD have developed two versions, which both look at the way current develops in time influenced by the charge

drift. For example, GERDA has developed a classifier based on the time evolution of the ratio $\frac{A}{E}$ of the amplitude of the current, A, and the energy released, related to the signal integral E in the BEGe. For a given process (e.g., a supposed $0\nu2\beta$ signal), the time profiles are markedly different on account of the position where the energy deposition occurs in the crystal. However, with a weighting potential uniform enough, as the one of Figure 3, about 90% of the trajectories result in the same time pattern. Such a pattern is dominated by the hole current, weak for most of the volume and increased only once the holes go inside the intensified field around the p^+ electrode. The electron current is negligible. With this approximation, the overall current profile, for the same integrated charge, will be different for the SSE and MSE, which makes $\frac{A}{E}$ a powerful tool against backgrounds. See Figure 4. A good discussion on the PSD for $0\nu2\beta$ experiments can be found in [16].

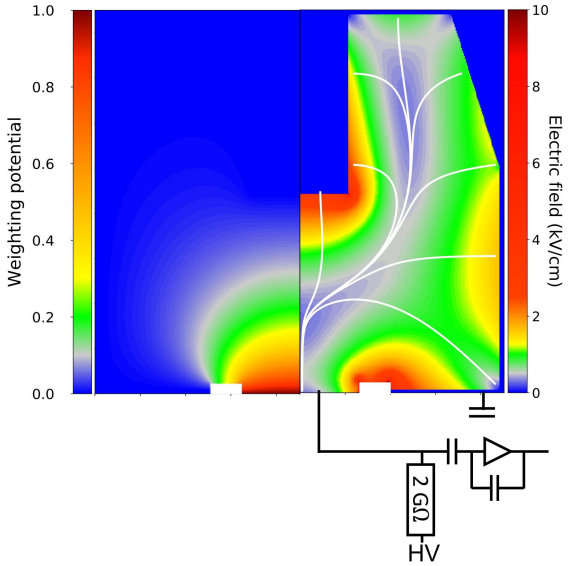

Figure 3. Weighting potential (**left**) and simulated total electrical field distribution (**right**) of an ICPC detector. The white lines show some simulated charge carrier paths using the ADL software. Taken from [16].

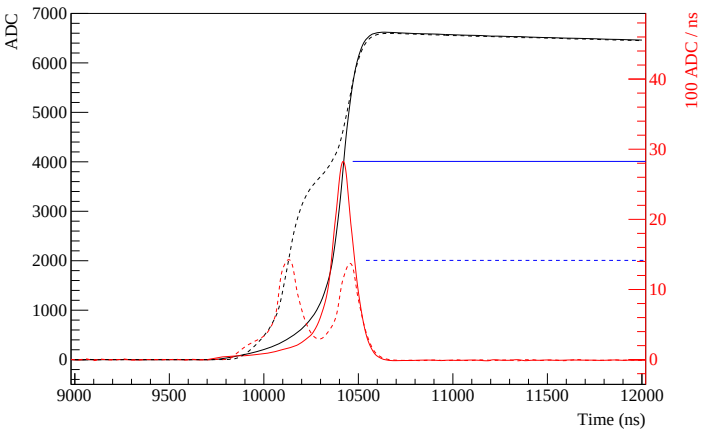

Figure 4. Shown in black are example SSEs (solid) and MSEs (dashed) from the 2615 keV ^{208}Tl peak for an enriched PPC detector. The current waveforms are shown in red with blue horizontal lines indicating their maximum value. Taken from [17].

4. Overview of the Past-Generation Experiments

In this section, we provide a description of the two "parent" experiments, which have set the landscape for the future with germanium in this field: GERDA and Majorana

Demonstrator. For each, we summarize their layout, the main backgrounds, and results, in terms of half-life.

4.1. GERDA

The Germanium Detector Array (GERDA) experiment has taken data until the end of 2019. Its data taking has run for several years, with a divide between a Phase 1 and a Phase 2 in 2013–2015. In Phase 1 the experiment collected 21.6 kg $\times$ y of exposure, while the total exposure at completion was of 104 kg $\times$ y. GERDA has provided the most stringent lower limit to date on the half-life of $0\nu2\beta$ from any isotope.

Since the LEGEND-200 design is largely based on the GERDA one, we chose to dwell mostly on GERDA. Of course, we highlight the MJD fundamental contributions to LEGEND-200 where relevant.

4.1.1. Description of the Apparatus

Arguably, the main success of GERDA is in having reduced its background index B at $Q_{\beta\beta}$ to only 5.2×10^{-4} counts/(keV $\times$ kg $\times$ y). The GERDA Collaboration managed to achieve such a low background rate primarily thanks to a very careful design of the detector, as shown in Figure 5.

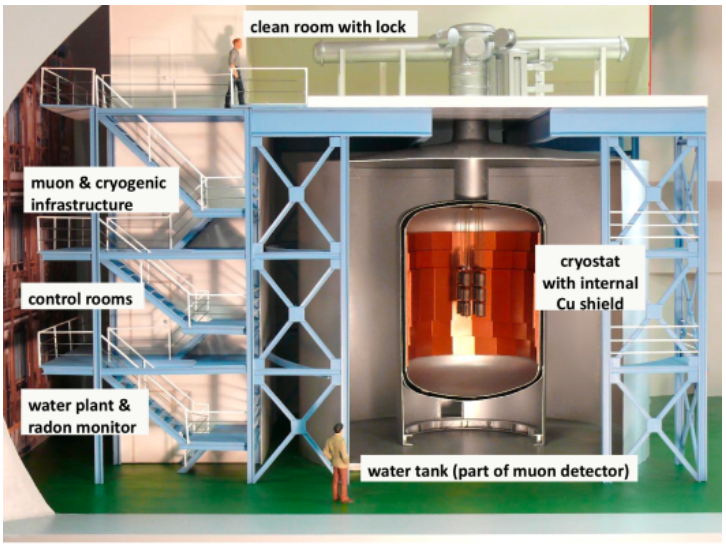

Figure 5. The GERDA detector, including the active veto, cryostat, and muon tank. Taken from [18].

The main features are:

- A segmented set of germanium diodes organized in strings for topological cuts, described in Section 3.3.1 in terms of the SSE and MSE;
- An innovative technique whereby the germanium diodes are immersed in a cryogenic liquid scintillator, namely 64 m^3 of Liquid Argon (LAr); this not only serves as a coolant for electronic noise reduction for the diodes, but is also instrumented for active background identification in their proximity.

While Phase 1 hosted only coaxial diodes, for Phase 2, 30 custom-designed BEGe-type diodes [19] were inserted. In total, 35.8 kg of germanium enriched at 88% in ^{76}Ge were used for the final result (seven of which were coaxial), organized into seven strings. An additional 7 kg of ICPC were attached in mid-2018, mainly for characterization in view of LEGEND [15].

A water pool of a capacity of 590 m^3 surrounding the cryostat ensured high efficiency against the prompt muon component of cosmic rays, based on the Cherenkov effect. The 128 nm scintillation light in the LAr was collected by 800 m of glass fibers coated in a Tetraphenyl Butadiene (TPB) wavelength shifter to match the spectral response of 90 Silicon Photomultipliers (SiPM) attached at the end. A nylon shroud was placed around each

string and coated with Wavelength Shifter (WLS), in order to isolate it from ^{42}K ions developed in the LAr and attracted to the n^+ dead layer, a background whose impact we describe in the following paragraph Section 4.1.2.

The core of the detector, with the strings, low-mass front-end electronics, and supports were dipped in LAr, all contained within a copper cylinder of 500 mm in diameter. At the top of the ≈2.2 m high structure, a feed-through for all the front-end electronics and a specialized charge sensitive pre-amplifier were placed, to herd the diode signals outside of the cryostat, into in-air electronics and digitizers.

A careful control of radioactive backgrounds was exercised when fabricating the materials, especially those of the suspenders, holders, and cables. Specialized screening techniques were deployed at various sites to measure the residual material and ambient radioactivity.

4.1.2. Main Background Sources

A vast documentation describing the background processes and their suppression and estimation is available from the GERDA Collaboration [20,21]. Here, we review the main sources of backgrounds experienced in GERDA, because they are the same one that LEGEND-200 and LEGEND-1000 will face.

Backgrounds can be divided essentially into three categories, mapping the nature of the radiation involved: α, β, and γ. In GERDA, the three are estimated to have about the same impact. The sources producing such radiation on or close to the diodes are grouped as follows:

- α generates a continuous background, which is mostly concentrated at high energies (up to about 5.5 MeV) and comes from the decay of ^{210}Po (τ = 138 d) from the ^{238}U decay chain happening on the diode surface. While the n^+ dead layer is too thick for a heavy particle such as an α to penetrate, some α are attracted electrically towards the thinner p^+ electrode by its strong electrical field and release energy inside the diode;
- β comes mainly from the decays of argon isotopes in the natural argon used for the veto. These are decays of ^{42}Ar into ^{42}K, where the positively-charged potassium ion is sometimes carried towards the n^+ electrode either by the diode electric field or, mechanically, by the convective motions in the LAr. Since $\tau(^{42}\text{K})$ = 12.4 h, it then β decays to excited states of ^{42}Ca near the diode, which can result in β electrons of up to 3.525 MeV energy penetrating the diode;
- It can also happen that $^{42}\text{Ca}^*$ de-excites by means of e.m. radiation, which results in specific γ lines visible in the diodes. That is part of a vaster suite of photon radiation, with energies falling within the GERDA analysis window E ∈ [1.93, 2.19] MeV. They include one line from the ^{214}Bi β decay (E_γ=2.119 MeV) and the Single Escape Peak (SEP) from ^{208}Tl at 2.104 MeV. To the origin of this radiation lie the various branches of ^{238}U and ^{228}Th decay chains from surrounding materials (such as cables and copper mounts). ^{40}K decays are also present in the material, but of low concern, as the corresponding γ energy from the electron capture is only 1460 keV;
- Finally, it is worth singling out some isotopes of cosmogenic activation that generate a flat background around $Q_{\beta\beta}$ and some nearby γ lines, namely ^{60}Co, activated from the copper in the supporting structures and surrounding shroud. Its rate is expected to contribute only ≈1% of the total B.

Interestingly, events of Double Escape Peak (DEP) from ^{208}Tl provide a distinctive signature (a peak at 1593 keV) that can be used to tune the PSD cut, since they behave as an SSE. MSEs have been considered from various Compton scattering regions, including the Compton continuum at $Q_{\beta\beta} \pm 35$ keV. A full γ spectrum in the vicinity of $Q_{\beta\beta}$ is shown in Figure 6, as taken by one of the ICPC detectors in GERDA.

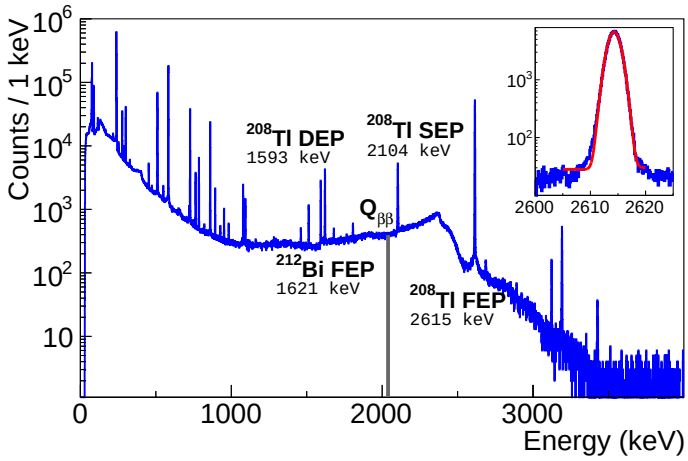

Figure 6. ^{228}Th spectrum taken with one of the GERDA ICPC detectors. The main γ lines, ^{208}Tl Double Escape Peak (DEP), ^{208}Tl Single Escape Peak (SEP), and ^{208}Tl and ^{212}Bi Full Energy Peak (FEP), used in the pulse analysis, are emphasized together with the $Q_{\beta\beta} \pm 35$ keV Compton continuum region. The inset shows a fit to the 2615 keV γ line. Taken from [15].

A number of mitigation techniques have been developed and deployed in time to reduce the above background events. Rather than looking at them in the context of GERDA, it is more interesting to see how the "germanium community" will make the most of such past experience to attain the desired sensitivity for LEGEND-200 and LEGEND-1000. We do so in Section 5.1.4. However, it is worth recalling here some important performance figures for the main background rejection techniques. The efficiency of the PSD cut to $0\nu2\beta$ events is around 69% for coaxial and around 90% for BEGe and the ICPC. The energy resolution at $Q_{\beta\beta}$ is (4.9 ± 1.4) keV FWHM for coaxial, (2.6 ± 0.2) keV FWHM for BEGe, and (2.9 ± 0.1) keV FWHM for the ICPC. The LAr veto efficiency to $0\nu2\beta$ events was estimated to be (97.9 ± 0.1)%, with an approximate dead time from the veto of around 2.2%. The veto provided a factor of six background reduction on top of the PSD. An exhaustive summary can be found in [6].

4.1.3. Results

A half-life lower limit was extracted from the combined Phase 1 and Phase 2 data, corresponding to an exposure of 127.2 kg $\times$ y. The limit coincides with the sensitivity, defined as the median expectation under the "no-signal" hypothesis. The limit of $T_{1/2} > 1.8 \times 10^{26}$ y (90% C.L.) [6] indicates an unprecedented low background in Phase 2 of $5.2^{+1.6}_{-1.3} \times 10^{-4}$ counts/(keV kg y). The mean background expected in the signal region ($Q_{\beta\beta} \pm 2\sigma$) is of 0.3 counts.

4.2. Majorana Demonstrator

The Majorana Demonstrator was a competitor of GERDA in the establishment of a low-background environment in view of a future ton-scale search. It took place at the Sanford Underground Research Facility (SURF) in the United States.

4.2.1. Description of the Apparatus

Different from GERDA, MJD used a conventional screening against radioactive and cosmic ray backgrounds by means of a passive material: it was surrounded by lead bricks. Two low-background copper cryostats contained the 29.7 kg of PPC detectors, hung into strings and surrounded by two layers of protecting copper shields. They were enriched at 88% in ^{76}Ge. Other than the same care as GERDA in material screening against radioactivity, particular care was used in fabricating the copper, electro-formed underground directly at SURF in dedicated baths, for minimum cosmogenic activation. The overall radioactivity of this copper is also estimated to be less than 0.3 µBq/kg from the ^{238}U and ^{228}Th decay

chains [22]. An active muon veto made of scintillating panels was also placed above the setup, which is shown altogether in Figure 7.

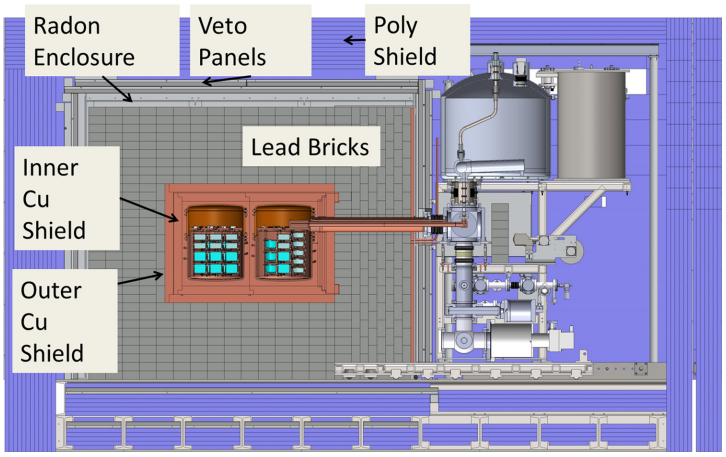

Figure 7. The schematics of the Majorana Demonstrator .

MJD managed to develop low-noise electronics, which affected positively its PSD capability and energy resolution. This is slightly better than the GERDA one (2.5 keV FWHM at $Q_{\beta\beta}$). The PSD, based on $\frac{A}{E}$, is $(90 \pm 3.5)\%$ efficient to SSE [23]. A complementary technique ("Delayed Charge Recovery" (DCR)) is used in MJD. It is based on α particles penetrating the active volume only through the thin passivated surfaces, where holes are strongly trapped. This generates a slower current turn-on, which can be used to identify α events.

4.2.2. Results

The combined PSD signal efficiency is about 80%. The corresponding background predicted in the ROI from the 360 keV window is around $Q_{\beta\beta}$ is $6.1 \pm 0.8 \times 10^{-3}$ counts/(keV kg y) [17]. Using 26 kg·y of exposure, the MJD provided a lower limit on the half-life of 2.7×10^{25} y (90% C.L.) with a median sensitivity of 4.8×10^{25} y (90% C.L.). More data are available to be analyzed for a "legacy" result.

5. What the Future (with Germanium) Holds: LEGEND

From such expertise and achievements stems LEGEND. The Collaboration's goal is to put together the best of both GERDA and MJD in terms of technology and know-how in order to promote the search for $0\nu2\beta$ with germanium all the way to a ton-scale detector. A two-stage approach has been devised, whereby a detector with 200 kg (LEGEND-200) will first take data for a few years, before leaving the stage to the full-fledged experiment of 1 t (LEGEND-1000). Together with the search per se, LEGEND-200 will also serve to qualify the development of large point-contact detectors such as the ICPC of 2–3 kg enriched to further than 90%, to prove a scalable layout and to test techniques for a very aggressive background reduction.

LEGEND-200 officially started its activities in 2020 and is hosted at LNGS, where it uses the GERDA infrastructure. It is due to be installed in summer/autumn 2021, with commissioning data taking to run until the end of the year and physics runs to start in 2022 with a completed detector mass in place in summer 2022.

In parallel, the R&D for LEGEND-1000 has started on several items, which we describe later. A phased production of larger ICPC detectors, assembly, and data taking with increasing germanium mass are expected to start around 2025–2026. A site for LEGEND-1000 has not yet been identified as of this publication. High-level contacts among the funding agencies of the countries interested in the project are taking place to determine the mutual level of commitment and contribution to LEGEND-1000 and identify a suitable site.

5.1. LEGEND-200

5.1.1. Description of the Apparatus

The LEGEND-200 detector inherits the GERDA infrastructure and is characterized as follows:

- Fourteen strings of the ICPC (about 140 kg), BEGe, and the PPC (altogether making the remaining approximate 60 kg), all enriched to 88% in ^{76}Ge and contained within one cylindrical volume surrounded by LAr;
- A 64 m^3, 4 m-diameter single cryostat with a lock system containing LAr, which serves both as the coolant and as the active veto close-by the diodes, thanks to the fibers and SiPM;
- All around the cryostat, a water tank, 10 m in diameter and 590 m^3 in capacity, will act as the muon veto, with PMTs detecting Cherenkov radiation from incoming cosmic rays.

A schematic view of the main pieces of LEGEND-200 is provided in Figure 8, which describes the GERDA setup.

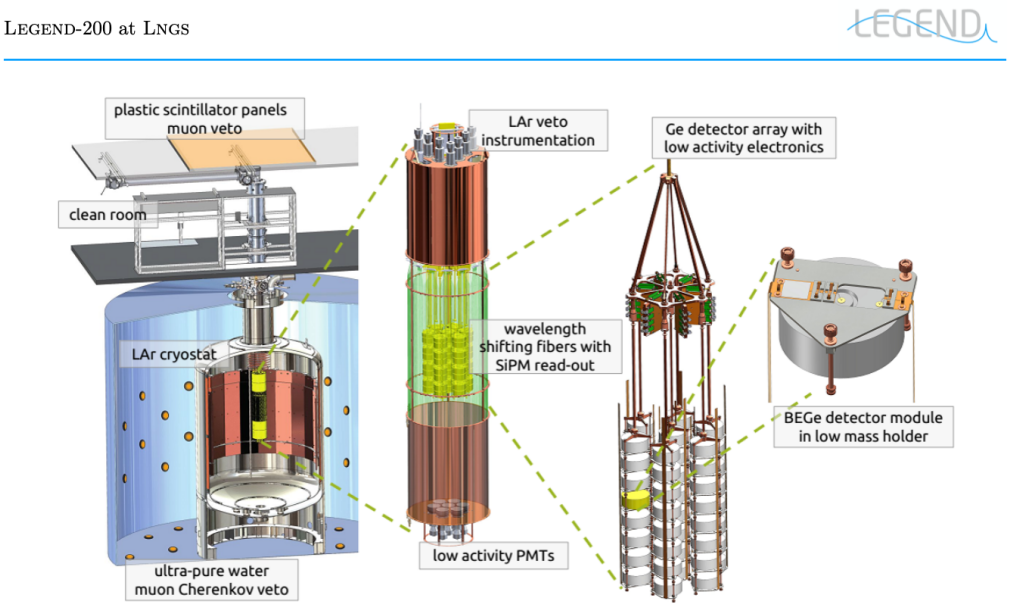

Figure 8. The schematics of the the GERDA detector at LNGS, with various steps of zooming from a general view closer to the detector string. It provides an idea of the LEGEND-200 setup.

5.1.2. New with Respect to the GERDA Infrastructure, in a Nutshell

- A new lock with an improved mechanics has been fit in to the cryostat and the clean room height increased for this purpose;
- New front-end (FE) electronics have been devised for both the diodes and the SiPM, in order to improve the signal-to-noise ratio (e.g., solutions closer to the MJD design, for the diode low-mass FE, new pre-amplifier to match the new LMFE, differential reading with coupled receiver and amplifier stage for the SiPM, new Flash-ADC);
- Improved light collection for the LAr veto system. A new system with a double curtain of optical fibers collects light more effectively, plus a wavelength-shifter-coated reflecting surface has replaced simple copper in the so-called "radon shroud" for maximum light collection.

More details on some of these are offered in the next section.

5.1.3. Energy Resolution

The energy resolution of the germanium detectors at $Q_{\beta\beta}$ is monitored regularly as batches are delivered for LEGEND-200. Preliminary results are condensed in Figures 9 and 10, which were obtained with 75.9 kg worth of detectors at the characterization facility in the HADES underground laboratory, in Belgium. They show that:

- The resolution at $Q_{\beta\beta}$ remains about constant as new detectors are produced. The mass-weighted average is 2.19 keV, even below the 2.5 keV level of MJD (see Figure 9);
- The resolution does not degrade with the detector mass, which bodes well for larger detector masses for LEGEND-1000 (see Section 3.3.1 and Figure 10).

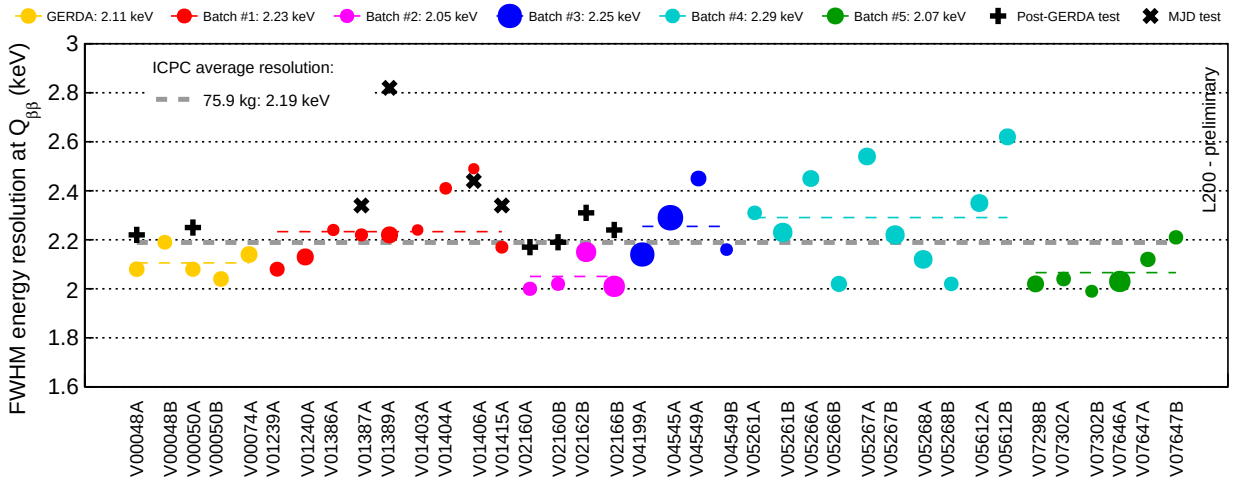

Figure 9. FWHM energy resolution of all LEGEND-200 ICPC detectors delivered to date, as measured in vendor vacuum cryostats (colored discs). The dashed lines indicate the mass-weighted average per production batch (colored) and for all detectors combined (gray). Each data point's diameter scales with its detector mass; uncertainties are on the order of or smaller than the marker sizes. Shown also are the values measured during testing in the GERDA (black plus) and Majorana Demonstrator (MJD, black cross) cryostats. From [24].

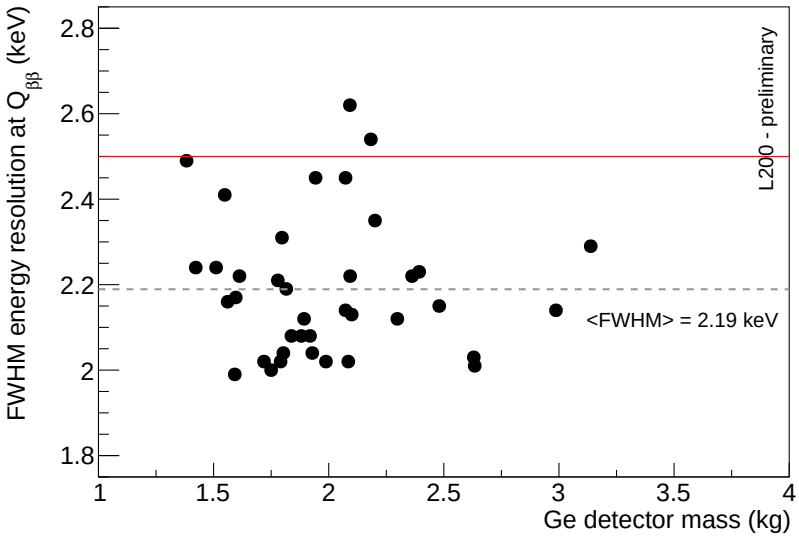

Figure 10. FWHM energy resolution of all LEGEND-200 ICPC detectors delivered to date, as measured in vendor vacuum cryostats, as a function of mass. Uncertainties are on the order of or smaller than the marker sizes. The dashed line indicates the overall weighted average and the solid red line the performance goal. From [24].

5.1.4. Background Control Measures

UGEF copper: The same level of care as in the past is being exercised in manufacturing radiopure materials. Detectors are mounted on low-mass holders in order to minimize the radioactivity around the diodes. All copper will be electro-formed underground. In addition to the MJD ones, three new baths were constructed at SURF to supply clean copper for the detector housing components of LEGEND-200 and LEGEND-1000.

PEN: The advancements in the understanding of postmachining contamination of plastics and metals will feed into the LEGEND-1000 effort of ultra-pure materials for the ultra-demanding background budget. One of such new plastics that are being machined to be used is Poly(Ethylene 2,6-Naphthalate) (PEN) [25]. This is an industrial polyester of good mechanical properties at the LAr temperature of 87 K (stronger than the silicon and copper it should replace). It scintillates in the optical blue region (peak of spectral response at 425 nm) and is capable of shifting the LAr light from 128 nm with a dominant decay constant of 34.91 ns [26]. It yields about one third of the light of conventional plastic scintillators and can be used as a self-vetoing material, in that it can detect and reveal its own radioimpurities [27]. A low (5–7 g) mass geometry has been optimized for LEGEND-200, which minimized the radioactivity load. In any case, as screened with the GeMPI screening facility at LNGS, it proved to meet the LEGEND-200 radio-purity requirements ($<$1 μBq/piece for ^{228}Ra and ^{228}Th). PEN pieces will replace the silicon plates that GERDA used as the detector and LMFE holders in between modules along a string. PEN holders have been successfully deployed in the so-called "post-GERDA test" in which some LEGEND developments and parts were tested at LNGS in the first half of 2020 (despite COVID-19), using the full GERDA infrastructure yet assembled. Further R&D is on-going for additional cleanliness and improved optical properties in view of an extended use in LEGEND-1000.

LAr: An active veto has proven very effective against specific backgrounds from ambient radioactivity and detector radioimpurities in GERDA (see Section 4.1.2). For this reason, LEGEND has adopted the strategy of a cryogenic liquid-based scintillation veto for both the 200 kg and 1000 kg phases. For LEGEND-200, two shrouds of fibers will be installed, tightly spaced and read out by 60 channels of front-end electronics (each reading nine SiPM in parallel). One SiPM array sees either end of a fiber bundle. A reflective foil coated with TPB has been installed in the area around the outer shroud for further reflection of optical photons back into the argon bath. This is applied on a new version of the "radon shroud" used to screen off radon nuclides from drifting into close contact with the diodes through the thermal convective modes of the argon. This enclosed region defines the "active volume" of the LEGEND-200 detector, the one where instrumentation is able to see light. Indicatively, a factor of 10 more light yield is expected to be seen from scintillation processes happening inside the active volume. LEGEND-200 has agreed with the argon gas supplier, LINDE, on a certified quality of the noble liquid supply. This "LEGEND" quality ensures a level of N_2 and O_2 pollutants in the argon around or below one part-per-million (ppm), with a particularly strong constraint on oxygen because of its effect on the suppression of the LAr scintillation output [28]. In order to maintain a high light yield and a good separation between the fast and slow component of the scintillation time profile, an even higher LAr purity is ensured by means of a dedicated purification plant. This uses a two-tier process, molecular sieves followed by copper shards, to filter out the remaining pollutants to less than 0.1 ppm. Sieves trap moisture and (some parts of) nitrogen, while the copper captures oxygen into an oxide. The purification is performed at first fill, with the plant placed just before the cryostat. Filling of the cryostat took place in the summer 2021. The possibility for recirculation of LAr in the purification plant during data taking is being considered, by equipping the cryostat with a pump to push LAr into the purification line continuously. Additionally, a dedicated device, called the LEGEND LAr Monitoring Apparatus (LLAMA), has been fit into the LEGEND-200 cryostat, far from the diode strings, to monitor the quality of the LAr in real time. It is composed of a γ source placed at the apex of a structure hosting trigger and read-out SiPM detectors at various

distances. A counting analysis at the expected γ energy of 60 keV is performed to extract the τ of the LAr triplet component and a reference light yield. LLAMA has operational since the start of filling and continuous data taking.

While all these provisions are expected to enhance the veto efficiency against external processes, they also increase the material placed around the diode strings. The main source of radioimpurity are the fibers: nuclides are believed to leak into the fiber machining during the cladding of the outer peel of a fiber. The background projections from such a source indicate meets the LEGEND-200 background budget, but mitigating measures are being undertaken in collaboration with fiber manufacturers to purify the production chain.

There is another source of background superimposing the external backgrounds: the high-activity β decays of the subdominant isotope ^{39}Ar (approximately 1.4 Bq/l measured by the WARP collaboration [29]). The ^{39}Ar β particle has a relatively low end-point at 600 keV; but because of its high activity, it can show up as a pile-up of two or more decays within one typical acquisition time window of a few microseconds, mimicking higher-energy background processes. For example, it interferes with the identification of delayed cosmic muon activation (e.g., neutron captures on ^{40}Ar with consequent de-excitation of ^{41}Ar). ^{39}Ar is hard to separate from natural argon, which means that one will have to both estimate its contribution statistically and find suitable ways to reject it on an event-by-event basis using multiplicity and topology in the LAr veto instrumentation.

5.1.5. Energy Calibration in LEGEND-200

The calibration of the energy response by the germanium detectors is performed by deploying radioactive sources at various points of the instrumented volume of LAr. 16 ^{228}Th sources ($T_{1/2}$ = 1.9 y, an activity of 5 kBq per source) have been produced and certified for use in the cryogenic environment. They are stowed away from the diodes during data taking and inserted by four dedicated motorized units for the periodic calibration runs. Figure 11 shows the design of the calibration source insertion system for LEGEND-200, which will be followed for LEGEND-1000.

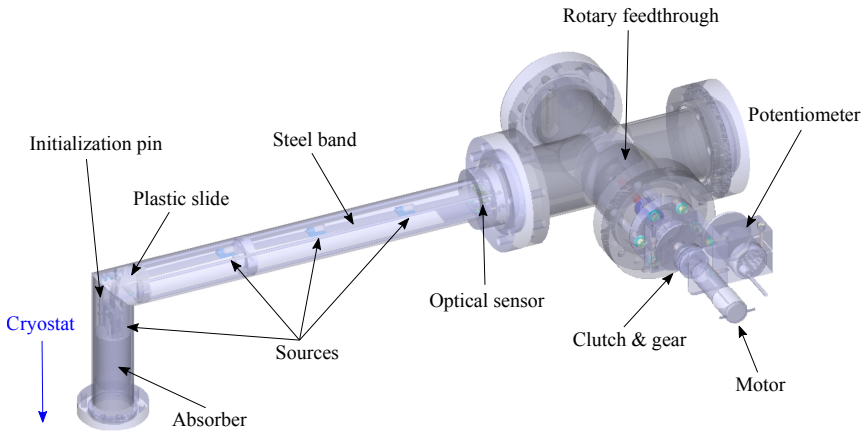

Figure 11. The schematics of the LEGEND-200 calibration source insertion system. From [24].

5.2. LEGEND-1000

An extensive review of the proposed baseline design, technical innovations, and physics reach of LEGEND-1000 has been released very recently [24]. This is based on certain assumptions for the hosting laboratory site (SNOLAB in Canada), but also explores alternatives (LNGS in Italy and SURF in the USA). The space that can be allocated to the detector dictates the design, while the site depth determines the cosmic ray rate and, therefore, the overall background index. At the time of writing, a site has not yet been determined to host LEGEND-1000, and the funding agencies are in contact in the USA and in Europe to establish the level of funding and in-kind contributions of the various countries to the experiment.

5.2.1. Current LEGEND-1000 Baseline Design

Based on the assumption that the experiment will take place at SNOLAB, the current baseline design is shown in Figure 12.

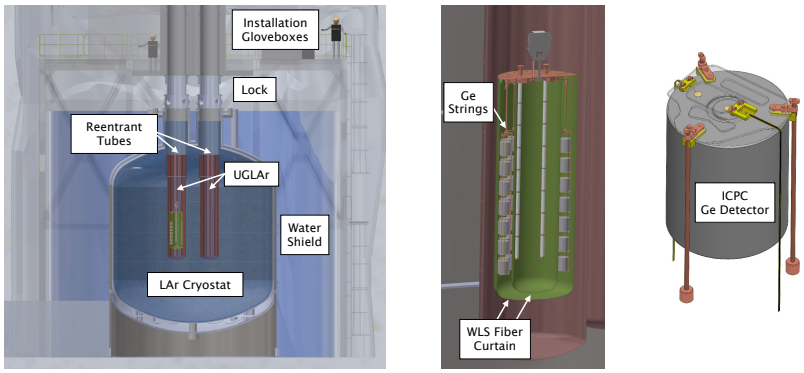

Figure 12. View and various elements of a baseline conceptual design of the LEGEND-1000 ^{76}Ge array that accommodates four 250 kg modules within a single vacuum-insulated LAr cryostat and water tank. From [24].

The design envisages a string unit replicated many times in four payloads, mechanically hosted in four corresponding re-entrant tubes. The tubes are immersed in a large cylindrical cryostat, with a 7 m inner diameter, optimized based on an assumed activity of the ^{232}Th from the stainless steel. In total, the cryostat holds 240 m^3 of coolant. The tubes are expected to host about 400 detectors overall: each re-entrant tube (made out of underground electro-formed copper) hosts 14 strings immersed in 3.3 m^3 of coolant. The re-entrant tubes have a 950 mm inner diameter. The baseline coolant is liquid argon. Different from LEGEND-200, however, in this case, the proposal is to fill the single payloads with the so-called Underground Liquid Argon (UGLAr) (see Section 5.2.2), while the volume outside of the tubes will be filled with ordinary, atmospheric argon. The cryostat is immersed in a water tank instrumented with photodetectors for additional γ and muon screening through the Cherenkov effect. However, this is reputed to be redundant to the LAr instrumentation alone at the SNOLAB depth and could be left out for the final design.

5.2.2. Underground LAr and Effect on the ^{42}K Background Reduction

UGLAr is argon not isolated from air by distillation, as is commercially done, but sourced from a deep underground CO_2 well. This argon will have not been exposed to cosmic rays and, therefore, is suppressed in argon isotopes generated from cosmogenic activation. It has been found [30] that UGLAr has a content of ^{39}Ar 1400-times less than atmospheric argon. A similar suppression is expected for ^{42}Ar, which is the parent of ^{42}K, a primary source of β and γ backgrounds in GERDA (see Section 4.1.2). For reference, the specific activity of ^{42}Ar in atmospheric argon is not well known, but several measurements with complementary techniques place it between about 40 µBq/kg and 170 µBq/kg. A summary of all such measurements was given by a recent paper [31].

LEGEND proposes to use some of the UGLAr that will be sourced in the URANIA plant at the Kinder Morgan Doe Canyon Facility in Cortez, CO, USA. This is a project developed by INFN in conjunction with the DarkSide-20k experiment to source UGLAr, which will then be purified of optical pollutants (especially O_2 and N_2) at the ARIA dedicated facility in Sardinia, Italy.

The overall production for DarkSide-50k is expected to be of 50 t and will take precedence. The estimate of the required contained mass of UGLAr for LEGEND-1000 is approximately 18 t and should be delivered in 2023. There is no foreseeable scenario where the URANIA UGLAr would not be available at all or that INFN would not make it available for LEGEND-1000. Furthermore, there are no known physical mechanisms that would trigger a more than negligible activation rate of UGLAr in the underground LEGEND-1000

setup. Therefore, the 1400 reduction factor is assumed as a baseline, and given the further possible purification in ARIA, the resulting background contribution of ^{42}K is taken as an upper limit. However, additional mitigation strategies are being considered in the event that one will have to resort to atmospheric argon. As already proven for GERDA [32], the use of thick nylon films all around each germanium string is effective in protecting the diode surface from potassium ion migration. Those shrouds are projected to reduce the ^{42}K contribution to the background rate by a factor of 100, at the price of adding themselves about 10^{-6} counts/(keV kg y) to the total background index B. They can be used together with, or in lieu of, underground argon supplies. Additional R&D worth mentioning in this context includes the encapsulation of detectors with PEN plastic to reduce the ^{42}K income.

5.2.3. Cosmic-Ray-Induced Background and Its Reduction

The penetrating muon component is the only one surviving the thick rock overburden that characterizes all candidate sites. The remainder of the filtered cosmic ray flux constitutes a background for $0\nu2\beta$ searches in two ways:

- A synchronous component (in time with the muon passage), also called "prompt", can traverse the LAr and the diodes, generating a spurious signal, which can be vetoed thanks to the LAr and/or water tank instrumentation;
- A delayed component, which is made of neutrons knocked off the argon by a passing muon, can generate spurious signals in the germanium diodes and in the liquid argon by capture and subsequent de-excitation. Particularly dangerous is the case of the postcapture formation of ^{77,m}Ge, where the ^{m} indicates that the isotope is metastable, with $T_{1/2} = 56$ s. Its de-excitation produces an SSE with about 150 keV of energy in 20% of cases.

SNOLAB has a depth of about six-thousand meter-water-equivalent (m.w.e.); LNGS is less deep, at about 3500 m.w.e., which translates into a flux about 100-times higher than at the former. At the reference SNOLAB depth, the total muon-induced contribution to the background index is expected to be $(6 \pm 6) \cdot 10^{-8}$ cts/(keV kg y). The two-order of magnitude gap at LNGS can be filled by adding a "virtual depth" effect looking at events with a certain time pattern and topology. The idea was first proposed in the context of GERDA [33], and it has now been updated for LEGEND-1000 [24]. The strategy is being optimized using simulations based on LEGEND-1000 detector geometries. It is expected that it will succeed in bringing the contribution of cosmogenic backgrounds to B to a manageable level for LNGS, also, making this a viable candidate site.

5.2.4. Total Background Index Projections for LEGEND-1000

The following projections on the background index levels stem from the above considerations on the backgrounds and how the design and careful choice of materials can mitigate their contribution around $Q_{\beta\beta}$. Among the many improvements at the center of the R&D activities in view of LEGEND-1000, it is worth mentioning the following:

- For the materials: clean manufacturing of alloys and plastics by laser excitation additive "3D printing" (SLA) and in-house synthesis of more radiopure PEN;
- For the electronics of the diodes: reduced front-end substrate and connector mass, related to new ASIC radiopure boards [34];
- All signal cables in the re-entrant tube made out of radiopure Kapton (including the diode high-voltage cables);
- For the liquid scintillator, veto variants include xenon-doped LAr to shift the light and reduce the attenuation and walls of SiPM instead of using the fibers if they cannot be made clean to the desired level of the backgrounds.

Figure 13 displays the values of the background index B estimated for all significant backgrounds for LEGEND-1000. Figure 14 illustrates the difference in level with respect to GERDA and how the reduction is intended to be attained. LEGEND estimates a final background index of $(9.1\ ^{+4.9}_{-6.3})\ 10^{-6}$ cts/(keV kg y) in LEGEND-1000.

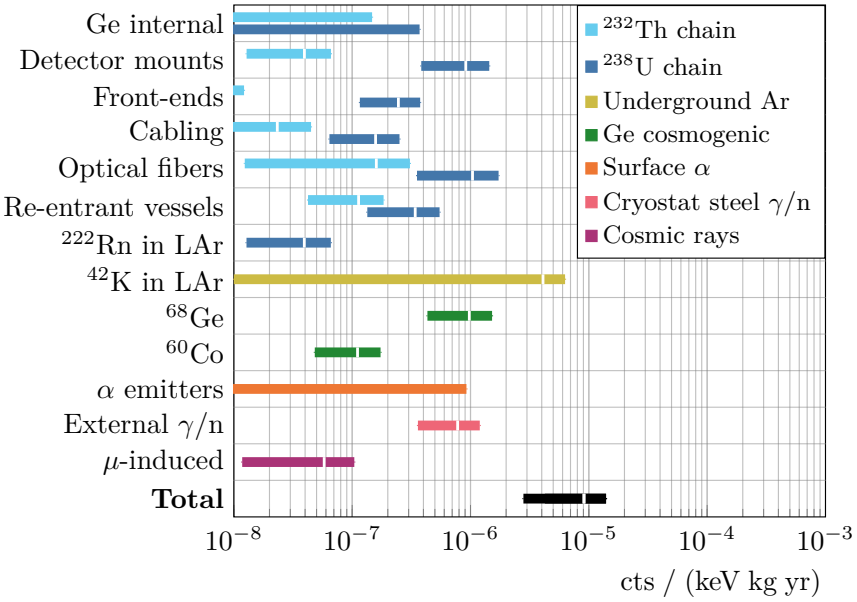

Figure 13. Background index estimated for the significant backgrounds expected for LEGEND-1000. Bands indicate 1-σ uncertainties (or 90% C.L. upper limits) due to the assay and simulation estimation of background-rejecting analysis cuts. For details of the calculation of these estimates, see [24].

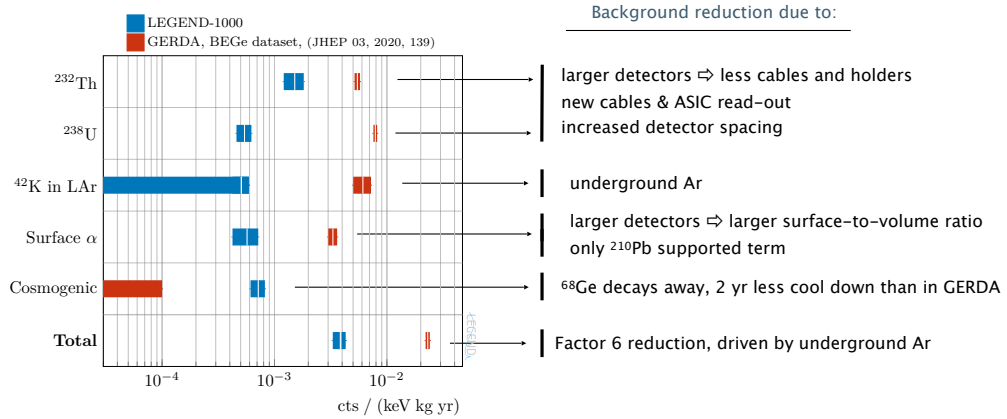

Figure 14. The expected background index associated with each of the dominant sources, before applying analysis cuts, projected for LEGEND-1000 (blue) and measured in GERDA (red). It illustrates the reduction power coming from a careful detector design and choice of materials. For details of the calculation of these estimates, see [24].

As said, α particles are able to propagate into the diode through the thin p^+ surface and passivated insulating grooves. The estimation of their contributed rate is hard to perform a priori, and the projections were taken from the experience accumulated in previous experiments. However, the PSD is very effective in rejecting them based on the principles introduced in Section 3.3.1. The survival probability after the PSD, as demonstrated by GERDA, is of about 10^{-3} (implied in Figure 14).

Assuming an FWHM energy resolution of 2.5 keV, the lower limit and 3-σ sensitivity to the $0\nu2\beta$ half-life of ^{76}Ge are shown in Figure 15.

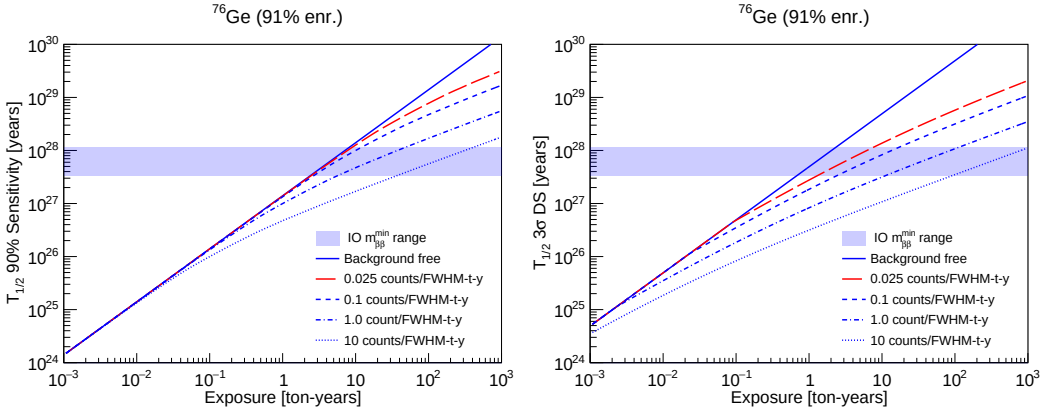

Figure 15. The sensitivity to a $0\nu2\beta$ decay signal in ^{76}Ge as a function of the exposure and background for a (left) 90% C.L. exclusion sensitivity and (right) 3σ (99.7% C.L.) Discovery Sensitivity (DS). The background rates are normalized to a 2.5 keV FWHM energy resolution.

6. Potential Technological Outcomes from LEGEND

As we tried to argue in this review, a large R&D effort has been made and continuous to be performed for the enhancement of the physics reach of LEGEND-200 and LEGEND-1000. This process could lead to the development of new pieces of technology or foster the advancement of emerging techniques in diverse applications. In particular, the work aimed at optimizing the LEGEND-1000 layout and reducing its background budget involves aspects such as:

- The search for materials with high mechanical and thermal resilience, which also have the property of scintillating to increase the light collection in the active veto and detect their own self-induced background radiation; this could improve the use of plastics in applied research and commercial applications (for example, as a thin support substrate in the developments of organic electronics such as organic diodes);
- Advancement of three-dimensional printing from resins (stereolithography or SLA) of radiopure plastics, in parallel with similar progress on metals such as copper; some groups from the U.S. and LNGS are already active with consistent expertise on this in LEGEND;
- Research on different schemes of wavelength shifting to dip or disperse in the liquid scintillator for a wider coverage and, consequently, enhanced light detection;
- Refined crystal growth in the industry for more uniform charge collection in larger germanium diodes, stemming from the LEGEND need for a highly performing PSD.

7. Expected Timeline of LEGEND-1000 and Conclusions

The LEGEND Collaboration just issued the cited preliminary Conceptual Design Report in parallel with presenting its case in a so-called "portfolio review" of the American DOE, which intends to establish a funding policy in the varied field of the search for $0\nu2\beta$. More such interactions are taking place in the coming months, for example at the end of the month of September 2021 between European and American funding agencies. Those consultations will influence the timeline for LEGEND-1000.

It is expected that the germanium enrichment and detector making would take a staged approach over 6 y. At the beginning, the detector production would proceed conservatively at a rate of 50 detectors per year, going up to 110 detectors per year as fabrication becomes more routine. At this rate, LEGEND-1000 would have sufficient mass for the first module after the first two years.

In conclusion, we presented a review of the past, present, and future of ^{76}Ge-based experiments in the search for $0\nu2\beta$. While this technique has yielded the most competitive results world-wide with GERDA and Majorana Demonstrator, LEGEND-200 promises to offer a stepping stone with various technical improvements to further reduce the background in view of the ton-scale stage. A diverse effort with many vibrant R&D activities is

taking place for LEGEND-1000 in order to meet the expectation that this still is the most competitive technique in the search for $0\nu2\beta$.

Author Contributions: N.B. focused on GERDA and on the description of germanium diodes and PSD. G.S. prepared the rest of the original draft, particularly focusing on LEGEND. All authors have read and agreed to the published version of the manuscript.

Funding: This research received no external funding.

Institutional Review Board Statement: Not applicable.

Informed Consent Statement: Not applicable.

Data Availability Statement: Data reported here are property of the experimental Collaborations.

Conflicts of Interest: The authors declare no conflict of interest.

References

1. CUPID Interest Group. CUPID pre-CDR. *arXiv* **2019**, arXiv:1907.09376.
2. Adhikari, G.; Kharusi, S.A.; Angelico, E.; Anton, G.; Arnquist, I.J.; Badhrees, I.; Bane, J.; Belov, V.; Bernard, E.P.; Bhatta, T.; et al. nEXO: Neutrinoless double beta decay search beyond 10^{28} year half-life sensitivity. *arXiv* **2021**, arXiv:2106.16243.
3. Fiorini, E.; Pullia, A.; Bertolini, G.; Cappellani, F.; Restelli, G. A search for lepton non-conservation in double beta decay with a germanium detector. *Phys. Lett. B* **1967**, *25*, 602–603. [CrossRef]
4. Aalseth, C.E.; Avignone, F.T., III; Brodzinski, R.L.; Cebrian, S.; Garcia, E.; Gonzalez, D.; Hensley, W.K.; Irastorza, I.G.; Kirpichnikov, I.V.; Klimenko, A.A.; et al. IGEX ^{76}Ge neutrinoless double-beta decay experiment: Prospects for next generation experiments. *Phys. Rev. D* **2002**, *65*, 092007. [CrossRef]
5. Klapdor-Kleingrothaus H.V.; Krivosheina I.V.; Dietz A.; Chkvorets O. Search for neutrinoless double beta decay with enriched ^{76}Ge in Gran Sasso 1990–2003 *Phys. Lett. B* **2004** *586*, 198-212. [CrossRef]
6. Agostini, M.; Benato, G.; Detwiler, J.A. Final Results of GERDA on the Search for Neutrinoless Double-β Decay. *Phys. Rev. Lett.* **2020**, *125*, 252502. [CrossRef] [PubMed]
7. Avignone, F.T., III; Elliott, S.R. The Search for Double Beta Decay With Germanium Detectors: Past, Present, and Future. *Front. Phys.* **2019**, *7*, 6. [CrossRef]
8. Kotila, J.; Iachello, F. Phase-space factors for double-β decay. *Phys. Rev. C* **2012**, *85*, 034316. [CrossRef]
9. Engel, J.; Menendez, J. Status and future of nuclear matrix elements for neutrinoless double-beta decay: A review. *Rep. Prog. Phys.* **2017**, *80*, 046301. [CrossRef] [PubMed]
10. Agostini, M.; Benato, G.; Detwiler, J.A. Discovery probability of next-generation neutrinoless double-β decay experiments. *Phys. Rev. D* **2017**, *96*, 053001. [CrossRef]
11. Agostini, M.; Bakalyarov, A.M.; Balata, M.; Barabanov, I.; Baudis, L.; Bauer, C.; Bellotti, E.; Belogurov, S.; Bettini, A.; Bezrukov, L.; et al. Probing Majorana neutrinos with double-β decay. *Science* **2019**, *365*, 1445–1448. [CrossRef]
12. Aghanim, N.; Akrami, Y.; Ashdown, M.; Aumont, J.; Baccigalupi, C.; Ballardini, M.; Banday, A.J.; Barreiro, R.B.; Bartolo, N.; Basak, S.; et al. Planck 2018 results: VI. Cosmological parameters. *A&A* **2020**, *641*, A6.
13. Angrik, J.; Armbrust, T.; Beglarian, A. KATRIN Design Report 2004. FZKA Scientific Report 7090. Available online: https://www.katrin.kit.edu/publikationen/DesignReport2004-12Jan2005.pdf (accessed on 15 September 2021).
14. Cooper, R.J.; Radford, D.C.; Hausladen, P.A.; Lagergren, K. A novel HPGe detector for gamma-ray tracking and imaging. *Nucl. Instrum. Methods Phys. Res. Sect. A Accel. Spectrometers Detect. Assoc. Equip.* **2011**, *665*, 25–32. [CrossRef]
15. Agostini, M.; Araujo, G.; Bakalyarov, A.M.; Balata, M.; Barabanov, I.; Baudis, L.; Bauer, C.; Bellotti, E.; Belogurov, S.; Bettini, A.; et al. Characterization of inverted coaxial ^{76}Ge detectors in GERDA for future double-β decay experiments. *Eur. Phys. J. C* **2021**, *81* , 505. [CrossRef]
16. Domula, A.; Hult, M.; Kermaïdic, Y.; Marissens, G.; Schwingenheuer, B.; Wester, T.; Zuber, K. Pulse shape discrimination performance of inverted coaxial Ge detectors. *Nucl. Instrum. Methods Phys. Res. Sect. A Accel. Spectrometers Detect. Assoc. Equip.* **2018**, *891*, 106–110. [CrossRef]
17. Alvis, S.I.; Arnquist, I.J.; Avignone, F.T., III; Barabash, A.S.; Barton, C.J.; Basu, V.; Bertr, F.E.; Bos, B.; Busch, M.; Buuck, M.; et al. Search for Neutrinoless Double-Beta Decay in ^{76}Ge with 26 kg y of exposure from the Majorana Demonstrator. *Phys. Rev. C* **2019**, *100*, 025501. [CrossRef]
18. The GERDA Experiment Official Website. Available online: https://www.mpi-hd.mpg.de/gerda/home.html (accessed on 12 September 2021).
19. Agostini, M.; Allardt, M.; Andreotti, E.; Bakalyarov, A.M.; Balata, M.; Barabanov, I.; Barros, N.; Baudis, L.; Bauer, C.; Becerici-Schmidt, N.; et al. Production, characterization and operation of ^{76}Ge enriched BEGe detectors in GERDA. *Eur. Phys. J. C* **2015**, *75*, 39. [CrossRef]
20. Agostini, M.; Allardt, M.; Andreotti, E.; Bakalyarov, A.M.; Balata, M.; Barabanov, I.; Barros, N.; Baudis, L.; Bauer, C.; Becerici-Schmidt, N.; et al. Background-free search for neutrinoless double-β decay of ^{76}Ge with GERDA. *Nature* **2017**, *544*, 47–52

21. Agostini, M.; Bakalyarov, A.M.; Balata, M.; Barabanov, I.; Baudis, L.; Bauer, C.; Bellotti, E.; Belogurov, S.; Bettini, A.; Bezrukov, L.; et al. Modeling of GERDA Phase II data. *J. High Energy Phys.* **2020**, *2020*, 139. [CrossRef]
22. Abgrall, N.; Arnquist, I.J.; Avignone, F.T., III; Back, H.O.; Barabash, A.S.; Bertr, F.E.; Boswell, M.; Bradley, A.W.; Brudanin, V.; Busch, M.; et al. The Majorana Demonstrator radioassay program. *Nucl. Instrum. Methods Phys. Res. Sect. A Accel. Spectrometers Detect. Assoc. Equip.* **2016**, *828*, 22–36. [CrossRef]
23. Alvis, S.I.; Arnquist, I.J.; Avignone, F.T., III; Barabash, A.S.; Barton, C.J.; Basu, V.; Bertr, F.E.; Bos, B.; Buuck, M.; Caldwell, T.S.; et al. Multisite event discrimination for the Majorana Demonstrator. *Phys. Rev. C* **2019**, *99*, 065501. [CrossRef]
24. Abgrall, N.; Abt, I.; Agostini, M.; Alexander, A.; Andreoiu, C.; Araujo, G.R.; Avignone, F.T., III; Bae, W.; Bakalyarov, A.; Balata, M.; et al. LEGEND-1000 Preconceptual Design Report. *arXiv* **2021**, arXiv:2107.11462.
25. Nakamura, H.; Shirakawa, Y.; Takahashi, S.; Shimizu, H. Evidence of deep-blue photon emission at high efficiency by common plastic. *EPL* **2011**, *95*, 22001. [CrossRef]
26. Wetzel, J.; TiraŞ, E.; Bilki, B.; Bostan, N.; KÖseyan, O.K. Scintillation timing characteristics of common plastics for radiation detection excited with 120 GeV protons. *Turk. J. Phys.* **2020**, *44*, 437. [CrossRef]
27. Majorovits, B.; Eck, S.; Fischer, F.; Gooch, C.; Hayward, C.; Kraetzschmar, T.; van der Kolk, N.; Muenstermann, D.; Schulz, O.; Simon, F. PEN as self-vetoing structural material. *AIP Conf. Proc.* **2018** *1921*, 090001.
28. Acciarri, R.; Antonello, M.; Baibussinov, B.; Baldo-Ceolin, M.; Benetti, P.; Calaprice, F.; Calligarich, E.; Cambiaghi, M.; Canci, N.; Carbonara, F.; et al. Effects of Nitrogen and Oxygen contamination in liquid Argon. *Nucl. Phys. B* **2009** *197*, 70–73 [CrossRef]
29. Benetti, P.; Calaprice, F.; Calligarich, E. Measurement of the specific activity of Ar-39 in natural argon. *NIM A* **2007** *574*, 83–88 [CrossRef]
30. Agnes, P.; Albuquerque, I.F.M.; Alexander, T.; Alton, A.K.; Araujo, G.R.; Ave, M.; Back, H.O.; Baldin, B.; Batignani, G.; Biery, K.; et al. DarkSide-50 532-day dark matter search with low-radioactivity argon. *Phys. Rev. D* **2018**, *98*, 102006. [CrossRef]
31. Ajaj, R.; Araujo, G.R.; Batygov, M.; Beltran, B.; Bina, C.E.; Boulay, M.G.; Broerman, B.; Bueno, J.F.; Burghardt, P.M.; Butcher, A.; et al. Electromagnetic backgrounds and potassium-42 activity in the DEAP-3600 dark matter detector. *Phys. Rev. D* **2019**, *100*, 072009. [CrossRef]
32. Agostini, M.; Barnabé-Heider, M.; Budjáš, D.; Cattadori, C.; Gangapshev, A.; Gusev, K.; Heisel, M.; Junker, M.; Klimenko, A.; Lubashevskiy, A.; et al. LArGe: Active background suppression using argon scintillation for the Gerda $0\nu2\beta$ experiment. *Eur. Phys. J. C* **2015**, *506*, 102006.
33. Wiesinger, C.; Pandola, L.; Schönert, S. Virtual depth by active background suppression: Revisiting the cosmic muon induced background of GERDA Phase II. *Eur. Phys. J. C* **2018**, *78*, 597. [CrossRef]
34. Edzards, F.; Willers, M.; Alborini, A.; Bombelli, L.; Fink, D.; Green, M.P.; Laubenstein, M.; Mertens, S.; Othman, G.; Radford, D.C.; et al. Investigation of ASIC-based signal readout electronics for LEGEND-1000. *J. Instrum.* **2020**, *15*, P09022. [CrossRef]